



Cite this: *Chem. Commun.*, 2022, 58, 2987

Received 21st December 2021,  
Accepted 4th February 2022

DOI: 10.1039/d1cc07162a

rsc.li/chemcomm

# Enhancing cellular sulfane sulfur through $\beta$ -glycosidase-activated persulfide donors: mechanistic insights and oxidative stress mitigation†

Prerona Bora, , Manjima B. Sathian and Harinath Chakrapani \*

**Sulfane sulfur species such as persulfides and polysulfides along with hydrogen sulfide protect cells from oxidative stress and are key members of the cellular antioxidant pool. Here, we report perthiocarbamate-based prodrugs that are cleaved by  $\beta$ -glycosidases to produce persulfide and relatively innocuous byproducts. The  $\beta$ -glucosidase-activated persulfide donor enhances cellular sulfane sulfur and protects cells against lethality induced by elevated reactive oxygen species (ROS).**

Redox-active species derived from sulfur play a central role in cellular signalling and metabolism, stress response and homeostasis.<sup>1</sup> Persulfides (RS-SH) and polysulfides (RS-(S)<sub>n</sub>-H), which are members of the sulfane sulfur pool, have emerged as important mediators in stress response.<sup>2,3</sup> Collectively, the sulfane sulfur pool together with hydrogen sulfide (H<sub>2</sub>S) is now considered a reservoir of antioxidant species that responds to oxidative stress and protects key cellular components from oxidative damage.<sup>4</sup> Hence, in addition to thiols such as glutathione and H<sub>2</sub>S, persulfides are summoned to counter stress caused by elevated reactive oxygen species (ROS). RS-SH is more nucleophilic than RSH as evidenced by a higher HOMO (51 kJ mol<sup>-1</sup> for CysS-SH vs. CysSH) leading to superior reactivity with electrophilic species.<sup>5</sup> Persulfides and polysulfides are also better at sequestering reactive oxygen species (ROS) and countering oxidative stress.<sup>6</sup> Protein persulfidation, which is an oxidative post translational modification of cysteine residues, not only contributes to redox signalling but also protects cysteines from irreversible oxidation.<sup>7</sup> Persulfides and polysulfides are excellent persulfidating agents compared to H<sub>2</sub>S and hence new strategies to enhance cellular persulfides responsive to fluoride,<sup>8</sup> esterase,<sup>9</sup> pH,<sup>10</sup> light,<sup>11</sup> H<sub>2</sub>O<sub>2</sub>,<sup>12,13</sup> and nitroreductase<sup>14</sup> have been developed. Recently, artificial substrates for 3-mercaptopyruvate sulfurtransferase (3-MST) as enhancers of cellular persulfides was reported.<sup>15</sup> Several of the aforementioned strategies have shown promise in

mitigating oxidative stress in cellular and animal models (Fig. 1a). However, several of them produce byproducts that are electrophilic, some have poor selectivity across cell types, many have diminished aqueous solubility, and in a few cases, no therapeutic relevance was demonstrated. Here, we report the design and development of a cell permeable  $\beta$ -glycosidase-activated persulfide donor that protects cells from oxidative stress.

$\beta$ -Glycosidases are a class of enzymes that cleave glycosidic bonds in oligo/polysaccharides. These enzymes are over-expressed in the gastrointestinal (GI) tract, especially the colon. Elevated levels of  $\beta$ -glycosidases are associated with certain pathophysiologies of the GI tract including inflammatory bowel disorder (IBD), Crohn's disease and ulcerative colitis and cancer.<sup>16,17</sup> Increased reactive oxygen species (ROS) leading to collateral damage of the tissue is common in these conditions.<sup>18</sup> Thus, enhancing antioxidants is a possible therapeutic approach for such conditions. Several colon-specific prodrug strategies that involve cleavage by  $\beta$ -D-glucosidase,  $\beta$ -D-galactosidase,  $\beta$ -D-xylosidase produced by the intestinal microflora are known.<sup>16,19</sup> Hence, taking the aforementioned aspects into consideration, we designed  $\beta$ -glycosidase-activated

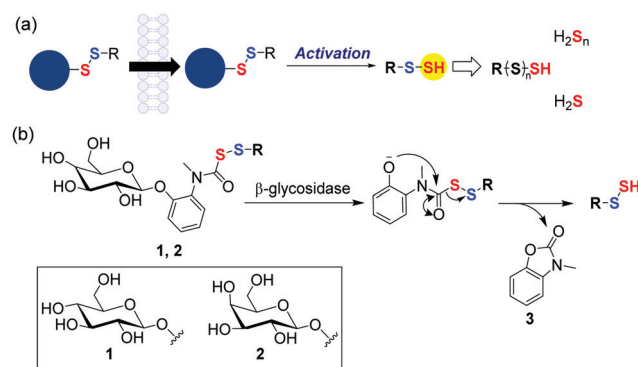


**Fig. 1** (a) Prodrug strategies to generate sulfane sulfur in cells. (b) Present work; prodrugs of persulfides/polysulfides cleavable by  $\beta$ -glycosidase (1:  $\beta$ -glucoside, 2:  $\beta$ -galactoside).

Department of Chemistry, Indian Institute of Science Education and Research Pune, Pune 411 008, Maharashtra, India. E-mail: harinath@iiserpune.ac.in

† Electronic supplementary information (ESI) available: Preparative methods, assay protocols and spectral data. See DOI: 10.1039/d1cc07162a

persulfide prodrugs (Fig. 1b); two series of compounds were considered: one cleavable by  $\beta$ -glucosidase (**1**) and the other by  $\beta$ -galactosidase (**2**). Being sugars, these compounds are expected to have enhanced aqueous solubility and would therefore have better applicability. Lastly, unlike certain other donors, once a persulfide is generated, no electrophilic and potentially toxic byproduct is formed.<sup>20</sup>

Compound **1a** (R = *N*-acetylcysteine methylester, Scheme 1) was synthesized in 5 steps (Scheme 1). First, the reaction of 2-nitrophenol with 2,3,4,6-tetra-*O*-acetyl- $\beta$ -D-glucopyranosyl bromide **4**, using a reported protocol<sup>21</sup> gave compound **5**. This was followed by reduction of the nitro group in **5** to its corresponding aniline **6** by using zinc in HCl. Formylation of the aniline followed by its reduction using borane dimethylsulfide<sup>22</sup> gave the *N*-methylaniline derivative **7**. In a separate reaction, *N*-acetylcysteine methylester (NACMe) was treated with chlorocarbonylsulfonyl chloride to obtain the *S*-perthiocarbonyl chloride **8a**, which was immediately reacted with compound **7** to obtain compound **9**.<sup>10</sup> Finally, deprotection of acetyl groups of **9** using sodium methoxide in methanol afforded **1a**.

To ascertain the reactivity of the compound towards  $\beta$ -glucosidase, **1a** was incubated with  $\beta$ -glucosidase in pH 7.4 phosphate buffer at 37 °C. LC/MS analysis of the reaction mixture revealed a complete decomposition of the compound within 10 h (Fig. 2a). A time course for this decomposition was obtained and curve fitting to a first order equation gave a rate constant of  $5.4 \times 10^{-3} \text{ min}^{-1}$  with a half-life of 128 min (Fig. 2a and Fig. S1, ESI†).

Under these conditions, as expected, the formation of *N*-methyl benzoxazolone byproduct (**3**) was observed with  $m/z = 150.0551 [\text{M} + \text{H}]^+$  (expected  $m/z = 150.0555$ ) (Fig. S2, ESI†). Curve fitting gave a rate constant of  $7.1 \times 10^{-3} \text{ min}^{-1}$ , which is comparable to the rate of decomposition of **1a** (Fig. 2b). Together, these data suggest that the cleavage step is the rate determining and once the sugar is cleaved, the release of the persulfide is fast. The ability of **1a** to generate persulfides under these conditions was next evaluated. A standard method for the characterization of persulfide species is to trap them with an electrophile to form a covalent adduct, which can be detected using HPLC or LC/MS.

*N*-(4-Hydroxyphenethyl)-2-iodoacetamide (HPE-IAM) has been previously reported<sup>23,24</sup> to be a potent and efficient persulfide/polysulfide alkylating agent (Scheme 2).<sup>25</sup> When **1a** was co-incubated in the presence of  $\beta$ -glucosidase and

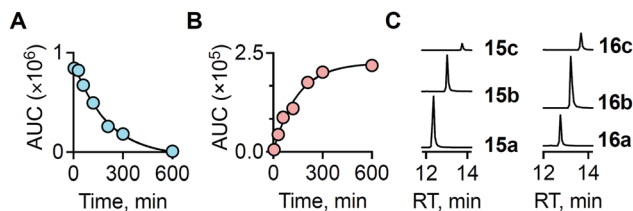
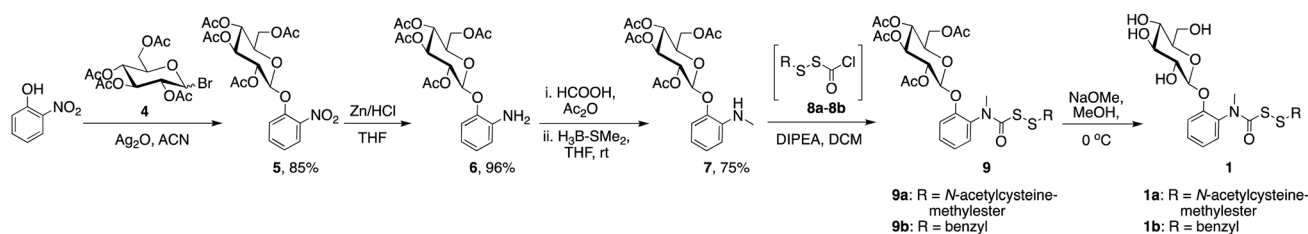


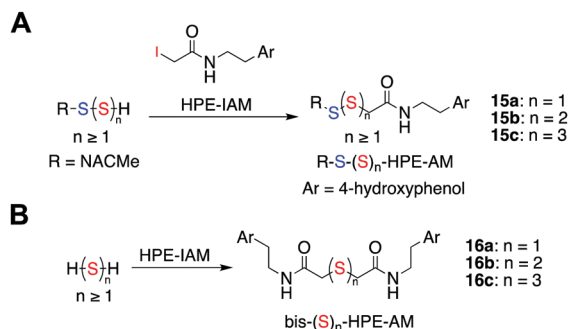
**Fig. 2** (a) Decomposition of **1a** upon incubation with  $\beta$ -glucosidase ( $10 \text{ U mL}^{-1}$ ) as monitored by LC/MS ( $m/z = 521.1250 [\text{M} + \text{H}]^+$ ; expected, 521.1264). Curve fitting to first order gave a rate constant of  $5.4 \times 10^{-3} \text{ min}^{-1}$ . (b) Formation of by-product **3** under the same conditions ( $m/z = 150.0551 [\text{M} + \text{H}]^+$ ; expected, 150.0555). Curve fitting to first order gave a rate constant of  $7.1 \times 10^{-3} \text{ min}^{-1}$ . (c) Extracted ion chromatogram of persulfides and polysulfides of *N*-acetylcysteine methylester (NACMe-S(<sub>n</sub>H)) generated from compound **1a**, detected as their HPE-AM adducts using LC/MS. **15a** ( $m/z = 387.1042 [\text{M} + \text{H}]^+$ ; expected, 387.1048); **15b** ( $m/z = 419.0781 [\text{M} + \text{H}]^+$ ; expected, 419.0769); **15c** ( $m/z = 451.0500 [\text{M} + \text{H}]^+$ ; expected, 451.0490). (d) Extracted ion chromatogram of hydrogen sulfide and hydrogen polysulfides detected as their bis-HPE-AM adducts. **16a** ( $m/z = 389.1545 [\text{M} + \text{H}]^+$ ; expected, 389.1535); **16b** ( $m/z = 421.1272 [\text{M} + \text{H}]^+$ ; expected, 421.1256); **16c** ( $m/z = 453.0991 [\text{M} + \text{H}]^+$ ; expected, 453.0976).

HPE-IAM, the appearance of a new peak at 12.36 min with  $m/z = 387.1042 [\text{M} + \text{H}]^+$  was observed that gradually increased over time (Fig. S3, ESI†). It was attributed as the NACMe persulfide adduct, **15a** (expected  $m/z = 387.1048$ ), thus confirming the generation of a persulfide under these conditions (Fig. 2c). We also found evidence for the formation of polysulfide adducts, **15b** and **15c** under these conditions (Fig. 2c). Additionally, appreciable amounts of  $\text{H}_2\text{S}$  as the bis-S-HPE-AM adduct (**16a**) with  $m/z = 389.1545 [\text{M} + \text{H}]^+$  (expected  $m/z = 389.1535$ ) was detected along with hydrogen polysulfides ( $\text{H}_2\text{S}_n$ ,  $n = 2$  and  $3$ ) (Fig. 2c). Furthermore, disulfide and trisulfide of NACMe were also detected (Fig. S4, ESI†). Together, these data demonstrate the ability of **1a** to produce a gamut of reactive sulfur species, hydrogen sulfide, persulfide and polysulfide.

Having confirmed the *in vitro* generation of persulfides/polysulfides from **1a**, we attempted to study its cell permeability and intracellular generation of sulfane sulfur. Human cytosolic  $\beta$ -glucosidase is present in significant concentrations in the liver, kidney, spleen and colon.<sup>26,27</sup> Human colon carcinoma (DLD-1) and hepatocarcinoma (HepG2) cell line were therefore used as model systems. A standard cell viability assay was conducted to assess the cytotoxicity of **1a** on DLD-1 and HepG2 cells. No significant toxicity was observed up to a concentration of  $100 \mu\text{M}$  (Fig. S5, ESI†). To detect intracellular sulfane sulfur,



**Scheme 1** Synthesis of glucopyranosyl derivatives, **1**.



**Scheme 2** (a) Reaction scheme showing detection of persulfides/polysulfides as their HPE-IAM adducts. Ar = 4-hydroxyphenol (b) hydrogen sulfide/polysulfides as their bis-S-HPE-IAM adducts.

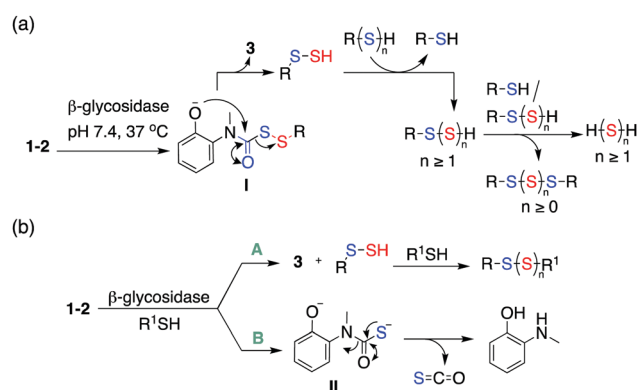
the persulfide probe SSP2 was used.<sup>28</sup> DLD-1 cells were pre-treated with SSP2 (50  $\mu\text{M}$ ) in the presence of CTAB (500  $\mu\text{M}$ ) followed by treatment with **1a**. A significant increment in the fluorescence signal corresponding to generation of sulfane sulfur was observed upon treatment with **1a** (Fig. S6, ESI<sup>†</sup>). The elevated concentration needed for enhancement of cellular persulfides is likely due to the diminished stability of persulfides in the reducing environment of the cells. Nevertheless, our data suggests that **1a** is cell permeable and is able to enhance the levels of intracellular sulfane sulfur pool.

Persulfides/polysulfides have previously been reported to have potent antioxidant effects and are efficient scavengers of ROS. Previously,  $H_2S$ -NSAID hybrids have been reported to have potent anti-inflammatory effects on models of colitis, attributable to  $H_2S$ .<sup>29</sup> In addition, COS/ $H_2S$  donors have shown to display cytoprotective effects against xenobiotic induced stress in colon cells.<sup>30</sup> To test the protective effects of persulfides/polysulfides in the colon against oxidative stress induced lethality, MGR-1, a cell permeable ROS generator was used to induce oxidative stress (Fig. S7, ESI<sup>†</sup>).<sup>31</sup> DLD-1 cells that were pre-treated with **1a** for 12 h were next exposed to MGR-1 for 4 h, following which cell viability was determined using a standard MTT assay. The assay indicates that **1a** was able to rescue cells from ROS induced lethality in a dose dependant manner. Under similar conditions, NAC failed to exhibit protective effects (Fig. S8a, ESI<sup>†</sup>). Next, to further corroborate our results, we used another cell line with an elevated expression of  $\beta$ -glucosidase, HepG2 cell line. When tested on HepG2 cells, similar results were obtained supporting the cytoprotective effects of the cell permeable persulfide donor **1a** (Fig. S8b, ESI<sup>†</sup>).

The next series of compounds (**2**) were designed to be cleaved by  $\beta$ -galactosidase. Our attempts to synthesize the galactopyranosyl derivative with NACMe persulfide **2a** (Fig. 1b;  $R = N$ -acetylcysteine methyl ester) were unsuccessful. The benzyl persulfide derivative **2b** was however synthesized (Fig. 1b,  $R = \text{Bn}$ ; Scheme S1, ESI<sup>†</sup>). The rate of cleavage of **2b** by  $\beta$ -galactosidase significantly faster than that of the  $\beta$ -glucoside by  $\beta$ -glucosidase (Fig. S9a; rate constant,  $6.8 \times 10^{-2} \text{ min}^{-1}$  and  $t_{1/2} = 10 \text{ min}$ , Fig. S9b, ESI<sup>†</sup>). The observed differences in the rates of cleavage by these enzymes is similar to previous

reports.<sup>32,33</sup> The byproduct **3** was observed under these conditions and its rate of formation was calculated to be  $8.6 \times 10^{-2} \text{ min}^{-1}$  (Fig. S10, ESI<sup>†</sup>). Upon co-incubation with  $\beta$ -galactosidase and HPE-IAM, as expected benzyl persulfide/polysulfide  $\text{Bn}(S)_n\text{SH}$  ( $n = 1-3$ ) along with the  $H_2S_n$  ( $n = 1-3$ ) adducts were detected (Fig. S11, ESI<sup>†</sup>). The compound **2b** was however found to be moderately cytotoxic when compared with **1a** (Fig. S12, ESI<sup>†</sup>). To verify if the benzyl persulfide contributed to cytotoxicity, the analogue **1b** was next synthesized by reacting **7** with the  $S$ -perthiocarbonyl chloride generated from benzyl mercaptan (**8b**) (Scheme 1). The decomposition profile of **1b** and persulfide/polysulfide generation profile of **1b** was comparable with that of **1a** (Fig. S13–S16, ESI<sup>†</sup>). The analogue **1b** was also found to be moderately cytotoxic in cells suggesting the importance of the functional group that is bound to the persulfide (Fig. S17, ESI<sup>†</sup>).

The following mechanism for the formation of persulfides/polysulfides from the glycopersulfide donors is proposed (Scheme 3a). The persulfide generators undergo decomposition in the presence of  $\beta$ -glycosidases to generate the intermediate phenolate **I**. Intramolecular cyclization of **I** produces a persulfide species along with the benzoxazolone byproduct **3**. The persulfide species once formed can further react with itself or reduced thiols to generate hydropolysulfide ( $\text{RSS}_n\text{H}$ ) species. Hydropolysulfides ( $\text{RSS}_n\text{H}$ ) upon reduction by thiols/persulfides would result in the generation of hydrogen polysulfide ( $H_2S_n$ ,  $n \geq 1$ ). A similar perthiocarbamate scaffold has been reported by Khodade *et al.* as precursors to persulfides that reacts with thiols to generate carbonyl sulfide (COS) as well.<sup>10</sup> COS undergoes hydrolysis to produce  $H_2S$  and this reaction is accelerated by carbonic anhydrase, an enzyme that is widely prevalent in cells.<sup>34</sup> Hence, in the presence of  $\beta$ -glycosidase and thiols, two possible parallel pathways **A** and **B** are possible (Scheme 3b). Pathway **A** indicates cleavage by  $\beta$ -glycosidase that forms the carbamate byproduct **3** with concomitant formation of persulfides/polysulfides. Pathway **B** indicates the cleavage of



**Scheme 3** (a) Proposed mechanism for the generation of persulfides and polysulfides from compounds **1-2** in the presence of  $\beta$ -glycosidases. (b) Major pathways for decomposition of **1** or **2** in the presence of a thiol and  $\beta$ -glycosidase. Pathway **A** involves decomposition by the enzyme while pathway **B** indicates disulfide bond cleavage by thiols to generate COS/ $H_2S$ .

the disulfide bond by thiols resulting in the generation of COS, which generates H<sub>2</sub>S.<sup>34</sup> The donor **2b** was examined for its reactivity towards biologically relevant thiols like *N*-acetyl cysteine (NAC) and glutathione (GSH) in the absence of an electrophile. When **2b** was co-incubated with  $\beta$ -galactosidase and NAC (5 equiv.) at 37 °C, if pathway **B** is significant, a reduction in the yield of **3** is expected. Indeed, when this reaction was conducted, a 25% reduction in the yield of the byproduct **3** was observed within 30 min (Fig. S18, ESI†). Mixed disulfides/polysulfides of NAC and benzyl (NAC-SS-Bn and NAC-(S)<sub>3</sub>-Bn) were also observed, which is indicative of pathway **A** (Scheme 3b and Fig. S19, ESI†). Whereas with GSH (10 equiv.), a 65% reduction in the formation of **3** was observed (Fig. S20, ESI†). The persulfide produced upon cleavage can also react with the prodrug *via* pathway **B**, forming COS. The derivative **1a** has a slower rate of cleavage by  $\beta$ -glucosidase derived from almonds with a half-life of 128 mins. Given the propensity of the compounds to react with thiols, it was envisaged that an important pathway for intracellular decomposition of **1a** would be pathway **B**. Previous reports show that human cytosolic  $\beta$ -glucosidases (hCBG) are more efficient at cleavage of  $\beta$ -glucosidic bonds compared to the enzyme derived from plants supporting the relevance of pathway **A** in mammalian cells.<sup>35</sup> Hence, our overall analysis suggests that the use of prodrugs developed herein results in the enhancement of cellular sulfur species, which have a protective effect against elevated ROS.

Financial support was from the Science and Engineering Research Board (CRG/2019/002900), Department of Science and Technology (PB, DST, INSPIRE Scheme), Department of Biotechnology (HC, BH/HRD/NBM-NWB/39/2020-21) and IISER Pune. DST Fund for Improvement of S&T Infrastructure (SR/FST/LSII-043/2016) to the IISER Pune Biology Department for setting up the Biological Mass Spectrometry Facility. The manuscript was written with inputs from all authors. PB and MBS carried out all experiments.

## Conflicts of interest

There are no conflicts to declare.

## Notes and references

- 1 T. V. Mishanina, M. Libiad and R. Banerjee, *Nat. Chem. Biol.*, 2015, **11**, 457.
- 2 M. R. Filipovic, J. Zivanovic, B. Alvarez and R. Banerjee, *Chem. Rev.*, 2018, **118**, 1253–1337.
- 3 C. Yang, N. O. Devarie-Baez, A. Hamsath, X. Fu and M. Xian, *Antioxid. Redox Signaling*, 2020, **33**, 1092–1114.
- 4 T. Zhang, H. Tsutsuki, K. Ono, T. Akaike and T. Sawa, *J. Clin. Biochem. Nutr.*, 2021, **68**, 5–8.
- 5 E. Cuevasanta, M. Lange, J. Bonanata, E. L. Coitiño, G. Ferrer-Sueta, M. R. Filipovic and B. Alvarez, *J. Biol. Chem.*, 2015, **290**, 26866–26880.
- 6 T. Ida, T. Sawa, H. Ihara, Y. Tsuchiya, Y. Watanabe, Y. Kumagai, M. Suematsu, H. Motohashi, S. Fujii, T. Matsunaga, M. Yamamoto, K. Ono, N. O. Devarie-Baez, M. Xian, J. M. Fukuto and T. Akaike, *Proc. Natl. Acad. Sci. U. S. A.*, 2014, **111**, 7606–7611.
- 7 J. Zivanovic, E. Kouroussis, J. B. Kohl, B. Adhikari, B. Bursac, S. Schott-Roux, D. Petrovic, J. L. Miljkovic, D. Thomas-Lopez, Y. Jung, M. Miler, S. Mitchell, V. Milosevic, J. E. Gomes, M. Benhar, B. Gonzalez-Zorn, I. Ivanovic-Burmazovic, R. Torregrossa, J. R. Mitchell, M. Whiteman, G. Schwarz, S. H. Snyder, B. D. Paul, K. S. Carroll and M. R. Filipovic, *Cell Metab.*, 2019, **30**, 1152–1170.
- 8 J. Kang, S. Xu, M. N. Radford, W. Zhang, S. S. Kelly, J. J. Day and M. Xian, *Angew. Chem., Int. Ed.*, 2018, **57**, 5893–5897.
- 9 Y. Zheng, B. Yu, Z. Li, Z. Yuan, C. L. Organ, R. K. Trivedi, S. Wang, D. J. Lefer and B. Wang, *Angew. Chem., Int. Ed.*, 2017, **56**, 11749–11753.
- 10 V. S. Khodade, B. M. Pharoah, N. Paolucci and J. P. Toscano, *J. Am. Chem. Soc.*, 2020, **142**, 4309–4316.
- 11 A. Chaudhuri, Y. Venkatesh, J. Das, M. Gangopadhyay, T. K. Maiti and N. D. P. Singh, *J. Org. Chem.*, 2019, **84**, 11441–11449.
- 12 P. Bora, P. Chauhan, S. Manna and H. Chakrapani, *Org. Lett.*, 2018, **20**, 7916–7920.
- 13 C. R. Powell, K. M. Dillon, Y. Wang, R. J. Carrazzone and J. B. Matson, *Angew. Chem., Int. Ed.*, 2018, **57**, 6324.
- 14 Y. Wang, K. M. Dillon, Z. Li, E. W. Winckler and J. B. Matson, *Angew. Chem., Int. Ed.*, 2020, **59**, 16698–16704.
- 15 P. Bora, S. Manna, M. A. Nair, R. R. M. Sathe, S. Singh, V. S. Sreyas Adury, K. Gupta, A. Mukherjee, D. K. Saini, S. S. Kamat, A. B. Hazra and H. Chakrapani, *Chem. Sci.*, 2021, **12**, 12939–12949.
- 16 D. R. Friend and G. W. Chang, *J. Med. Chem.*, 1984, **27**, 261–266.
- 17 H. Englyst, *FEMS Microbiol. Lett.*, 1987, **45**, 163–171.
- 18 H. Zhu and Y. R. Li, *Exp. Biol. Med.*, 2012, **237**, 474–480.
- 19 V. R. Sinha and R. Kumria, *Pharm. Res.*, 2001, **18**, 557–564.
- 20 The LD<sub>50</sub> of **3** has been found as 890 mg kg<sup>-1</sup> with no reported toxicity in mice, in *Registry of Toxic Effects of Chemical Substances*, ed. D. V. Sweet, US Department of Health and Human Services CDC, 1987.
- 21 X. Chen, X. Ma, Y. Zhang, G. Gao, J. Liu, X. Zhang, M. Wang and S. Hou, *Anal. Chim. Acta*, 2018, **1033**, 193–198.
- 22 I. Okamoto, M. Terashima, H. Masu, M. Nabeta, K. Ono, N. Morita, K. Katagiri, I. Azumaya and O. Tamura, *Tetrahedron*, 2011, **67**, 8536–8543.
- 23 H. A. Hamid, A. Tanaka, T. Ida, A. Nishimura, T. Matsunaga, S. Fujii, M. Morita, T. Sawa, J. M. Fukuto, P. Nagy, R. Tsutsumi, H. Motohashi, H. Ihara and T. Akaike, *Redox Biol.*, 2019, **21**, 101096.
- 24 T. Numakura, H. Sugiura, T. Akaike, T. Ida, S. Fujii, A. Koarai, M. Yamada, K. Onodera, Y. Hashimoto, R. Tanaka, K. Sato, Y. Shishikura, T. Hirano, S. Yanagisawa, N. Fujino, T. Okazaki, T. Tamada, Y. Hoshikawa, Y. Okada and M. Ichinose, *Thorax*, 2017, **72**, 1074–1083.
- 25 T. Akaike, T. Ida, F.-Y. Wei, M. Nishida, Y. Kumagai, M. M. Alam, H. Ihara, T. Sawa, T. Matsunaga, S. Kasamatsu, A. Nishimura, M. Morita, K. Tomizawa, A. Nishimura, S. Watanabe, K. Inaba, H. Shima, N. Tanuma, M. Jung, S. Fujii, Y. Watanabe, M. Ohmura, P. Nagy, M. Feilisch, J. M. Fukuto and H. Motohashi, *Nat. Commun.*, 2017, **8**, 1177.
- 26 B. Hultberg and P. A. Öckerman, *Clin. Chim. Acta*, 1970, **28**, 169–174.
- 27 H. M. M. Arafa, *Eur. J. Pharmacol.*, 2009, **616**, 58–63.
- 28 W. Chen, C. Liu, B. Peng, Y. Zhao, A. Pacheco and M. Xian, *Chem. Sci.*, 2013, **4**, 2892.
- 29 S. Fiorucci, S. Orlandi, A. Mencarelli, G. Caliendo, V. Santagada, E. Distrutti, L. Santucci, G. Cirino and J. L. Wallace, *Br. J. Pharmacol.*, 2009, **150**, 996–1002.
- 30 P. Chauhan, K. Gupta, G. Ravikumar, D. K. Saini and H. Chakrapani, *Chem. – Asian J.*, 2019, **14**, 4717–4724.
- 31 D. S. Kelkar, G. Ravikumar, N. Mehendale, S. Singh, A. Joshi, A. K. Sharma, A. Mhetre, A. Rajendran, H. Chakrapani and S. S. Kamat, *Nat. Chem. Biol.*, 2019, **15**, 169–178.
- 32 T. B. Cai, D. Lu, X. Tang, Y. Zhang, M. Landerholm and P. G. Wang, *J. Org. Chem.*, 2005, **70**, 3518–3524.
- 33 E. Calatrava-Pérez, S. A. Bright, S. Achermann, C. Moylan, M. O. Senge, E. B. Veale, D. C. Williams, T. Gunnlaugsson and E. M. Scanlan, *Chem. Commun.*, 2016, **52**, 13086–13089.
- 34 C. P. Chengelis and R. A. Neal, *Toxicol. Appl. Pharmacol.*, 1980, **55**, 198–202.
- 35 S. Tribolo, J.-G. Berrin, P. A. Kroon, M. Czjzek and N. Juge, *J. Mol. Biol.*, 2007, **370**, 964–975.